Emergent RNA-RNA interactions can promote stability in a nascent phototrophic endosymbiosis

Benjamin H. Jenkins[1,2]*, Finlay Maguire[3], Guy Leonard[1,2], Joshua D. Eaton[1], Steve West[1], Benjamin E. Housden[1], David, S. Milner[1,2], & Thomas A. Richards[1,2]*

[1]Living Systems Institute and Biosciences, University of Exeter, Devon EX4 4QD, UK

[2]Department of Zoology, University of Oxford, 11a Mansfield Road, Oxford OX1 3SZ, UK

[3]Faculty of Computer Science, Dalhousie University, 6050 University Ave, Halifax NS B3H 1W5, Canada

*Correspondence: thomas.richards@zoo.ox.ac.uk & ben.jenkins@zoo.ox.ac.uk

KEYWORDS

Paramecium bursaria, algae, mutualism, symbiosis, RNAi, Dicer, RDR, siRNA

ABSTRACT

Eukaryote-eukaryote endosymbiosis was responsible for the spread of chloroplast (plastid) organelles. Stability is required for the metabolic and genetic integration that drives the establishment of new organelles, yet the mechanisms which act to stabilise nascent endosymbioses – between two fundamentally selfish biological organisms – are unclear. Theory suggests that enforcement mechanisms, which punish misbehaviour, may act to stabilise such interactions by resolving conflict. However, how such mechanisms can emerge in a nascent endosymbiosis has yet to be explored. Here, we propose that endosymbiont-host RNA-RNA interactions, arising from digestion of the endosymbiont population, can result in a cost to host growth for breakdown of the endosymbiosis. Using the model nascent endosymbiosis, *Paramecium bursaria* – *Chlorella* spp., we demonstrate that this mechanism is dependent on the host RNA-interference (RNAi) system. We reveal through small RNA (sRNA) sequencing that endosymbiont-derived mRNA released upon endosymbiont digestion can be processed by the host RNAi system into 23-nt sRNA. We predict multiple regions of shared sequence identity between endosymbiont and host mRNA, and demonstrate through delivery of synthetic endosymbiont sRNA that exposure to these regions can knock-down expression of complementary host genes, resulting in a cost to host growth. This process of host gene knock-down in response to endosymbiont-derived RNA processing by host RNAi factors, which we term 'RNAi-collisions', represents a

mechanism which can promote stability in a nascent eukaryote-eukaryote endosymbiosis. By imposing a cost for breakdown of the endosymbiosis, endosymbiont-host RNA-RNA interactions may drive maintenance of the symbiosis across fluctuating ecological conditions and symbiotic status.

SIGNIFICANCE STATEMENT

Stable endosymbiosis between eukaryotic microbes has driven the evolution of further cellular complexity. Yet the mechanisms which can act to stabilise a nascent eukaryote-eukaryote endosymbiosis are unclear. Using the model nascent endosymbiotic system, *Paramecium bursaria–Chlorella*, we demonstrate that endosymbiont-host RNA-RNA interactions can drive a cost to host growth upon endosymbiont digestion, punishing the host for misbehaviour. These RNA-RNA interactions are facilitated by the host RNA-interference system. For endosymbiont mRNA sharing a high-level of sequence identity with host transcripts, this process can result in host gene knock-down. We propose that these endosymbiont-host RNA-RNA interactions–'RNAi collisions'–represent a viable enforcement mechanism to sanction the host for breakdown of the endosymbiosis, promoting the stability of a nascent endosymbiotic interaction.

MAIN TEXT

A nascent endosymbiosis between eukaryotes was a pre-requisite for the spread of photosynthetic organelles, such as plastids[1–5]. This transition from transiently engulfed cells to obligate organelles is driven by metabolic and genetic integration. Yet, to become manifest, a stable intermediary state must exist upon which this process of integration can proceed[1,3,5–8]. Conflict is an inevitable outcome of all symbioses, the resolution of which can significantly impact the stability of an interaction. Enforcement mechanisms which punish misbehaviour can act to stabilise symbioses[9,10], yet we know little about how these can emerge in a nascent endosymbiotic interaction. *Paramecium bursaria* – a ciliate protist which harbours a clonal population of intracellular green algae, *Chlorella* spp.[11–13] – represents a tractable model system to study emergent mechanisms in a nascent endosymbiosis[14]. The interaction is facultative[11,14–17] and based on two-way metabolic exchange[18–25]. Endosymbiotic algae are housed within modified host phagosomes called perialgal vacuoles, which may be fused with host lysosomes to trigger digestion[26] allowing *P. bursaria* to maintain control over the interaction in the event of conflict[27–29]. However, it is

62 unclear how this endosymbiotic system is protected from over-exploitation by the host
63 which would ultimately lead the interaction to collapse[30–35].

64 RNA-RNA interactions can play a role in host-pathogen symbiotic systems[36–40],
65 whereby RNA can 'hi-jack' the small interfering RNA (siRNA) pathway of the symbiotic
66 partner to modulate expression of genes involved in virulence or alternatively resistance.
67 Whether analogous RNA-RNA interactions could occur in an endosymbiotic system has yet
68 to be elucidated. The presence of a functional siRNA pathway in *Paramecium*, and its role in
69 RNA-interference (RNAi), has been validated as a tool for gene silencing in both *Paramecium*
70 *bursaria*[41] and non-photo-endosymbiotic congener, *Paramecium tetraurelia*[42–46]. RNAi can
71 be initiated through the provision of bacterial food transformed to express double-stranded
72 RNA (dsRNA) with high sequence similarity to a target transcript[41,43]. *Paramecium* can also
73 process single-stranded RNA (ssRNA) – including ribosomal RNA (rRNA) and messenger RNA
74 (mRNA) – derived from a prokaryotic cell acquired through phagotrophy[42]. This processing is
75 mediated by conserved RNAi protein components which also function in endogenous
76 transcriptome regulation[41,42,44,47]. Significantly, these studies propose that mRNA, derived
77 both exogenously[41,42] and endogenously[41,44], can act as substrates for siRNA generation in
78 *Paramecium*.

79 We demonstrate that RNA released upon digestion of the algal endosymbiont is
80 processed by the host RNAi system in *P. bursaria*. For endosymbiont-derived mRNA sharing
81 a high-level of sequence identity with host transcripts, this processing may interfere with
82 endogenous host gene expression resulting in a cost to host growth (**Fig. S1**). We track the
83 interaction through sRNA sequencing, recapitulate the effect through exposure to synthetic
84 endosymbiont RNA, and demonstrate that this mechanism is mediated by host Dicer, Piwi,
85 Pds1 and RdRP proteins. This process of host gene knock-down in response to
86 endosymbiont-derived RNA processing by host RNAi factors, which we term 'RNAi-
87 collisions', represents a candidate enforcement mechanism which can promote stability in a
88 nascent eukaryote-eukaryote endosymbiosis. By imposing a cost for breakdown of the
89 endosymbiosis, endosymbiont-host RNA-RNA interactions may drive maintenance of the
90 symbiosis across fluctuating ecological conditions and symbiotic status.

91 ***Endosymbiont digestion in P. bursaria results in an RNAi-mediated 'physiological cost' to***
92 ***the host***

93 *P. bursaria* can be purged of endosymbiotic algae via treatment with the ribosomal
94 translational inhibitor, cycloheximide[14]. A comparison of ribosomal protein (RP) L29A
95 predicted protein sequences, the active site of cycloheximide function, confirmed that
96 *Paramecium* possess a specific nucleotide polymorphism identified as a determinant of
97 cycloheximide resistance in other species (**Fig. S2**). This substitution was absent in all green
98 algal species assessed, including known algal endosymbionts of *P. bursaria*. Upon treatment
99 with cycloheximide, a significant reduction in algal-chlorophyll fluorescent intensity per host
100 cell was observed after two-to-three days (**Fig. 1A**). A clear de-coupling of host *P. bursaria*
101 cell number and algal fluorescence was also observed, consistent with translational
102 inhibition in the algae but not the host (**Fig. S2**), demonstrating that loss of a photosynthetic
103 endosymbiont population does not immediately result in a decline in host cell number.
104 Additional staining with LysoTracker Green to identify acidic vacuoles, including lysosomes,
105 revealed that this loss of algal fluorescence was linked to increased lysosomal activity in the
106 host cytoplasmic environment (**Fig. 1B**). These data support that elimination of the
107 endosymbiotic algal population during cycloheximide treatment[14,26] is triggered by host
108 digestion.

109 Continued treatment with cycloheximide resulted in a significant retardation to *P.*
110 *bursaria* culture growth, however this same effect was not observed in the non-photo-
111 endosymbiotic congener species, *P. tetraurelia* (**Fig. 1C**). Both *Paramecium* species harbour
112 the same cycloheximide resistance conferring substitution in RPL29A (**Fig. S2**), suggesting
113 that elimination of endosymbiotic algae is costly to *P. bursaria* culture growth. Loss of algal
114 derived photosynthate and plastid derived metabolites represents an obvious cost.
115 However, we sought to explore whether a part of this cost may be attributed to host
116 exposure to endosymbiont-derived RNA during digestion of the endosymbiont population,
117 and whether this cost was mediated by the host RNAi system.

118 Knock-down of *Dcr1* (a host-encoded endoribonuclease Dicer required for siRNA
119 generation) through complementary dsRNA exposure significantly rescued the cost to *P.*
120 *bursaria* culture growth associated with cycloheximide treatment (**Fig. 1D** and Fig. S3). This
121 was consistent with *Dcr1* (Dicer) knock-down in a prior study attenuating the effect of *E. coli*
122 vector-based RNAi feeding in *P. bursaria*[41]. In the aforementioned study, knock-down of
123 host-encoded *PiwiA1, PiwiC1* (AGO-Piwi effectors required for targeted RNA cleavage) and

124 *Pds1* (a *Paramecium*-specific component with an unknown but essential role in exogenously
125 induced RNAi) also attenuated an *E. coli*-vector feeding-based RNAi effect[41]. Here, knock-
126 down of host-encoded *PiwiA1* and *Pds1* similarly rescued the cost to *P. bursaria* culture
127 growth associated with cycloheximide treatment (**Fig. 1E** and Fig. S3). Involvement of *Pds1*
128 confirms that the observed RNAi effect is mediated by the host, as no identifiable
129 homologue of *Pds1* could be identified in the green algal genomes and transcriptomes
130 sampled[41,48]. Furthermore, it excludes the possibility that off-target effects arising from host
131 Dicer knock-down, including potential compensatory function of additional Dicer or Dicer-
132 like paralogues in *P. bursaria*[41], could be responsible for the RNAi effect observed. The near
133 complete rescue observed upon partial knock-down of Dicer suggests that host Dicer
134 processing, rather than loss of algal derived metabolites, is a more significant factor relating
135 to growth retardation under these conditions. Taken together, these data suggest that the
136 physiological cost to *P. bursaria* growth incurred during cycloheximide treatment, in which
137 the endosymbiotic algae are being broken down and digested by the host, is mediated by
138 host-encoded RNAi components. These data support the occurrence of RNAi-mediated RNA-
139 RNA interactions between endosymbiont and host.

140 **Endosymbiont breakdown triggers an abundance of Dicer-dependent endosymbiont**
141 **derived sRNA within *P. bursaria***

142 To investigate the occurrence of RNA-RNA interactions between endosymbiont and host, we
143 tracked the abundance of endosymbiont-derived, host-processed sRNA in *P. bursaria* during
144 endosymbiont digestion. Disruption of host RNAi was achieved through partial knock-down
145 of Dicer, allowing us to directly test for an increase in endosymbiotic algal-derived 23-nt
146 sRNA (the size associated with host Dicer processing[41,42,49]) resulting from cycloheximide
147 induced endosymbiont breakdown. Upon treatment with cycloheximide, we identified an
148 increased abundance in all 21-29 nt reads mapping to endosymbiont-derived mRNA over
149 two-to-three days (**Fig. 2A** and **Fig. S4**). This same trend was observed for reads mapping to
150 algal endosymbiont rRNA-derived sRNA (**Fig. S5**). Reads were mapped with 100% identity,
151 allowing no mismatches. Any reads that additionally mapped to the host with 100% identity
152 were removed, to ensure that the subset of sRNA detected was of definitive algal origin. A
153 significant increase in algal mRNA-derived 23-nt sense and antisense sRNA demonstrates a
154 greater abundance of potential RNAi substrates during endosymbiont digestion[41,42,49].

155 Partial knock-down of host Dicer during cycloheximide treatment significantly ablated
156 this endosymbiont mRNA-derived 23-nt antisense abundance after three days of
157 cycloheximide treatment (**Fig. 2B** and **Fig. S4**). This suggests that an increase in
158 endosymbiont mRNA-derived 23-nt antisense sRNA during endosymbiont digestion is
159 dependent on host Dicer function. This is consistent with knock-down of host Dicer
160 specifically reducing 23-nt sRNA abundance in *Paramecium*[41,42,49], and the observation that
161 *Paramecium* RNAi factors are capable of processing both endogenously and exogenously
162 derived mRNA[42,44]. It is important to note that this effect likely under-represents the full
163 extent of host Dicer processing, due to the requirement for a paradoxical and therefore
164 incomplete Dicer perturbation through Dicer-dependent RNAi-based knock-down[41].
165 Furthermore, these data represent only a subset of the sRNA potentially present due to the
166 stringent mapping approach used to identify endosymbiont-derived sRNA, as any reads that
167 additionally mapped to host RNA template with 100% sequence identity in either
168 orientation were excluded from this analysis. While these reads with high shared sequence
169 identity are the most important subset of sRNA for the identification of putative mRNA-
170 mRNA interactions between endosymbiont and host, their exclusion here has allowed us to
171 identify host RNAi processing of definitively endosymbiont-derived transcripts. Interestingly,
172 one of the host-derived transcripts that mapped with 100% identity to an excluded
173 endosymbiont-derived 23-nt sRNA was *P. bursaria* heat shock protein 90 (*HSP90*). An
174 investigation of regions of high shared sequence identity between endosymbiont and host is
175 explored below.

176 Next, we conducted a series of control observations. Firstly, we assessed whether
177 cycloheximide treatment was altering general host-derived sRNA production, despite the
178 inferred host resistance discussed above (**Fig. S2**). Reads were mapped to a dataset of 20
179 host transcripts that contained no potential 23-nt overlap with any identified algal
180 transcripts (allowing for ≤2-nt mismatches), to ensure that these host transcripts were
181 unaffected by an increased rate of putative RNA-RNA interactions derived from the
182 endosymbiont (**Fig. S6**). No significant increase in 23-nt abundance was observed for reads
183 mapping to this subset of host mRNA transcripts during cycloheximide treatment, consistent
184 with host resistance to cycloheximide not altering the host-derived population of sRNAs
185 with low sequence identity to algal mRNA. Secondly, we assessed whether endosymbiotic

186 algal strains cultured under free-living conditions would also generate an abundance of 23-
187 nt sRNA upon cycloheximide treatment (**Fig. S7**). Importantly, no clear increase in 21-25 nt
188 algal-derived sRNA abundance was observed during algal treatment with cycloheximide
189 when grown outside of the host cytoplasmic environment, nor was a 23-nt peak in algal
190 derived sRNAs evident. This is consistent with data from a previous study which found that
191 the algal endosymbiont of *P. bursaria* was not actively generating sRNA >20-nt[41]. These
192 results suggest that increased algal endosymbiont-derived 23-nt sRNA abundance upon
193 treatment with cycloheximide is dependent on host sRNA processing within the
194 endosymbiotic system. Taken together, these data indicate that an abundance of
195 endosymbiont-derived RNAs are released during endosymbiont digestion, which then act as
196 substrate for processing by the host RNAi system, resulting in 23-nt sRNAs. Importantly,
197 processing of endosymbiont-derived sRNA in a host Dicer-dependent manner indicates that
198 these interactions are occurring in the host cytoplasm, supporting the hypothesis that
199 endosymbiont-host mRNA-mRNA interactions are possible.

200 **Comparison of transcriptome data reveals the potential for host transcript interaction by**
201 **endosymbiont-derived RNAs**

202 To understand the extent of possible RNA-RNA interactions between endosymbiont and
203 host, we built a bioinformatic transcriptome processing tool, eDicer
204 (https://github.com/fmaguire/eDicer), which allows identification of all possible Dicer-
205 generated sense and antisense oligonucleotides produced from a given transcriptome
206 dataset. By mapping 23-nt reads to a second ('host') dataset allowing for ≤2-nt mismatches,
207 potential RNA-RNA interactions between an input (endosymbiont, vector, or food) and a
208 host RNA population can be identified. Inclusion of reads with ≤2-nt mismatches were based
209 on the tolerance for mismatching complementarity reported during RNAi-mediated knock-
210 down of gene expression in multiple systems[50–54]. Confirmation of a similar mismatch
211 tolerance in *P. bursaria* is shown in **Fig. 3E** & **Fig. S12**. For a full overview of the eDicer
212 comparative analysis process, please refer to the **Supplementary Methods**.

213 Using a dataset consisting of transcripts binned as either 'endosymbiont' or 'host'
214 (using a curated *P. bursaria* transcriptome[55]), we identified 35,703 distinct 23-nt putative
215 mRNA-mRNA interactions between the *P. bursaria* 'host' and 'endosymbiont' RNA
216 populations, representing 0.121% of the total inventory of distinct host 23-nt k-mers

217 identified (**Fig. S8A**; see also **Table S2** & **Supplementary Methods**). This was found to be
218 120-fold greater than the number of putative 23-nt mRNA-mRNA interactions predicted
219 between bacterial food and host transcripts (from two different bacterial sources).
220 Furthermore, the ratio of total:'potentially-lethal' putative 23-nt mRNA-mRNA interactions
221 (determined by cross-referencing genes known to be conditionally essential in
222 *Saccharomyces cerevisiae*[56]) was found to be greater between endosymbiont-and-host
223 transcripts (1:1.4) than between bacterial food-and-host transcripts (1:0.16/0.17). Similar
224 patterns were observed for predicted rRNA-rRNA interactions (**Fig. S8B,** see also **Table S2** &
225 **Supplementary Methods**). These *in silico* analyses demonstrate that there is far greater
226 potential for the occurrence of both mRNA-mRNA and rRNA-rRNA interactions between the
227 algal endosymbiont and host (eukaryote-eukaryote) RNA populations, than there is between
228 bacterial food and host (prokaryote-eukaryote) RNA populations.

229 ***In vivo* exposure to a synthetic endosymbiont mRNA-derived chimera generates knock-**
230 **down of high-identity host transcripts**

231 Having identified the occurrence of putative endosymbiont-host RNA-RNA interactions *in*
232 *silico*, we assessed whether exposure to synthetic fragments of algal mRNA could
233 recapitulate the cost to host growth observed during endosymbiont digestion (**Figure 1E**).
234 We identified ten endosymbiont mRNA interaction fragments that shared >91% (or 21-nt)
235 sequence identity with host transcripts across a 23-nt region, selected at random from the
236 analysis reported in **Fig. S8A**. Each mRNA interaction fragment was chosen to contain at
237 least 1 SNP specific to the endosymbiont to ensure that any identifiable effect could be
238 attributed to an endosymbiont-like transcript, rather than the host version. These
239 interaction fragments were predicted to still be effective RNAi templates for *P. bursaria*
240 based on the tolerance for mis-matching complementarity observed in RNAi-mediated
241 knock-down in other systems[50–54] (and confirmed below in *P. bursaria*; **Fig. 3E** & **Fig. S12**).
242 Six mRNA interaction fragments showed putative homology to 'non-lethal' yeast genes
243 (including *EF1-*α and *HSP90*); two showed putative homology to 'lethal' yeast genes
244 (including *tub-*β); and the remaining two had no identifiable homologues in yeast (**Table S1**).
245 Significantly, *HSP90* was the host transcript previously identified as a candidate for putative
246 endosymbiont-host RNA-RNA interaction in the sRNA analysis of **Fig. 2**. However, to ensure
247 that any identifiable effect could be attributed to the endosymbiont-derived transcript, the

248 newly identified interaction fragment was chosen from a different region of this gene
249 containing 2 SNPs specific to the endosymbiont. All ten mRNA interaction fragments were
250 composed of the predicted interacting 23-nt sRNA sequence (**Fig. S8A**) flanked by 11-nt of
251 contiguous 'non-hit' endosymbiont transcript as a filler on each side (**Table S3**). These ten
252 45-nt fragments were combined into a single 450-nt synthetic endosymbiotic algal chimera
253 (**Fig. 3A**), cloned into an L4440 plasmid, and transformed into *E. coli* for feeding-induced
254 RNAi.

255 Exposure to endosymbiotic algal chimera dsRNA resulted in significant retardation of
256 *P. bursaria* culture growth (**Fig. 3B**). Once more, this effect was attenuated by knock-down
257 of host Dicer, demonstrating an RNAi-mediated response to synthetic endosymbiont-host
258 mRNA-mRNA interactions that resembled the host response to endosymbiont digestion in
259 **Fig. 1C-E**. It is important to note that synthetic exposure to endosymbiont-derived RNA via
260 an *E. coli* feeding vector would likely over-represent these putative RNA interactions.
261 However, to address this issue, we designed a non-hit 'nonsense' control composed of a
262 tandem assembly of the 11-nt regions of contiguous 'non-hit' algal transcript present in the
263 chimera. A relative dilution of endosymbiont chimera dsRNA delivery alongside the
264 'nonsense' control (1, 1:1 and 1:3) also resulted in *P. bursaria* culture growth retardation
265 (**Fig. S9**), demonstrating that a reduced relative delivery of synthetic endosymbiont RNA can
266 also result in a cost to host growth. Similar experiments were conducted to investigate the
267 possibility of endosymbiont-host rRNA-rRNA interactions, but showed that there was no
268 equivalent effect on host growth, suggesting that ribosomal RNA is shielded from such
269 effects (**Fig. S10**, see also **Table S4**).

270 To identify which putative mRNA-mRNA interactions were capable of facilitating a cost
271 to *P. bursaria* culture growth, we identified the ten 450-nt host transcripts predicted to be
272 hit by each endosymbiont derived 23-nt mRNA interaction fragment used in the chimera
273 (**Figure 3C** - three examples are shown). Individual exposure to dsRNA corresponding to
274 each individual but longer *P. bursaria* transcript-form identified three which resulted in a
275 significant cost to host growth, relative to Dicer knock-down controls (**Fig. 3D**; see **Fig. S11**
276 for all 10). These *P. bursaria* transcripts correspond to elongation factor-1α (*EF-1α*), heat
277 shock protein 90 (*HSP90*; the host transcript identified as a candidate for putative
278 endosymbiont-host RNA-RNA interaction in the sRNA analysis of **Fig. 2**), and tubulin-β chain

279 (*tub-β*). It can therefore be inferred that these are the 23-nt mRNA interaction fragments
280 (**Fig. 3A/C**) that likely resulted in a cost to host growth observed during synthetic
281 endosymbiont chimera dsRNA exposure (**Fig. 3B**). Using mRNA extracted from *P. bursaria*
282 during chimera-RNAi feeding described above (**Fig. 3B**), qPCR revealed a reduction in host
283 transcript expression of *EF-1α* and *tub-β* in response to endosymbiont chimera dsRNA
284 exposure (**Fig. 3E**). Host transcript expression of *HSP90* appears inconclusive, however,
285 expression of all three host transcripts was partially rescued upon knock-down of host Dicer
286 (**Fig. S12**). From these data we can therefore conclude that 23-nt of >91% complementary
287 'endosymbiont' transcript is sufficient to facilitate detectable knock-down of a
288 corresponding host transcript, demonstrating that exposure to endosymbiont-derived RNA
289 originating from phagosomes is capable of impacting host gene expression via host RNAi
290 knock-down.

291 It is important to consider that delivery of a synthetic endosymbiont-derived RNA
292 chimera represents only an approximation of the putative 23-nt RNA-RNA interactions
293 occurring in *P. bursaria*. Exposure to endosymbiont RNA via an *E. coli* feeding vector would
294 likely over-represent these putative interactions. However, the random generation of 23-nt
295 Dicer substrates across the dsRNA chimera (only three regions of which resulted in a
296 detectable cost to host growth; **Fig. 3A/D** & **Fig. S11**) represents only part of the wider *E.*
297 *coli*-derived RNA population processed by the host RNAi system during chimera-RNAi
298 feeding. Together with dilution of endosymbiont chimera dsRNA delivery (**Fig. S9**), these
299 observations support the hypothesis that only a relatively small number of 23-nt RNA-RNA
300 interactions can induce a cost to host growth in *P. bursaria.* Furthermore, these data
301 confirm that sRNAs with ≤2-nt mismatches are effective templates for RNAi-mediated
302 knock-down of gene expression in *P. bursaria*, suggesting that the sRNA analysis in **Fig. 2**
303 may under-represent the true scale of endosymbiont-derived sRNAs that can result in RNA-
304 RNA interactions between endosymbiont and host. Importantly, we note that the
305 occurrence of putative endosymbiont-host RNA-RNA interactions does not exclude a wider
306 cost to host growth arising from processing a large population of algal derived RNAs with no
307 defined host target, a process which must pose a cost to host cellular economics and
308 transcriptional control/fidelity. For further justification of this 'synthetic' approach, and a
309 consideration of the results that we can reliably draw from these data, see **Discussion S1**.

310 **Single-stranded delivery of synthetic endosymbiont-derived RNA, analogous to**
311 **endosymbiont mRNA, results in a cost to *P. bursaria* growth**

312 As RNA derived naturally from the endosymbiont was unlikely to be double-stranded, two
313 further constructs were designed to assess the efficacy of synthetic endosymbiont chimera
314 single-stranded RNA (ssRNA) exposure in *P. bursaria* (**Fig. 4** & **Fig. S13**). Exposure to
315 endosymbiont chimera ssRNA also resulted in a significant cost to *P. bursaria* culture
316 growth, however this effect was only observed when delivered in the sense orientation
317 ([+]ssRNA). Notably, chimera [+]ssRNA exposure resulted in a greater cost to host growth
318 than chimera dsRNA exposure. A similar orientation bias was observed upon Dicer knock-
319 down during cycloheximide treatment in a prior experiment, in which delivery of Dicer
320 [+]ssRNA rescued culture growth to a greater extent than delivery of Dicer [-]ssRNA or Dicer
321 dsRNA (**Fig. S14**). Importantly, the orientation of [+]ssRNA represents the same orientation
322 as the mRNA transcripts from which each of these target templates were identified.

323 Knock-down of host Dicer (dsRNA delivery) was able to attenuate the cost to host
324 growth associated with endosymbiont chimera [+]ssRNA exposure (**Fig. 4**). Importantly,
325 simultaneous knock-down of host *Rdr1* and *Rdr2* (RNA-dependent RNA polymerases
326 involved in amplification of primary or secondary sRNA triggers during RNAi[42,46]) also
327 significantly rescued this cost to host growth. This is consistent with the role of RdRP
328 proteins in processing exogenous sRNA, partially degraded mRNA cleavage products, or full-
329 length mRNA transcripts in *Paramecium*[42,44–46]. As for Dicer, knock-down of host RdRP
330 through RNAi represents a potential paradox, and so constitutes only partial or transient
331 loss of function[41]. However, we are again confident that disruption in this manner would be
332 sufficient to perturb RdRP-mediated RNAi in *P. bursaria* after 14 days, as seen in **Fig. 4**.
333 While the mechanism of down-stream Dicer processing of RdRP-generated dsRNA
334 substrates remains unknown (see **Discussion S1**), we can nonetheless infer from these data
335 that single-stranded RNA-induced RNAi knock-down in *P. bursaria* is partially dependent
336 upon host RdRP function.

337 Irrespective of the mechanistic basis for a sense oriented ssRNA knock-down bias, it is
338 important to note that delivery of chimera [+]ssRNA demonstrated here represents the
339 same orientation as the endosymbiont derived mRNA interaction fragments from which
340 these putative endosymbiont-host RNA-RNA interactions were identified. This is consistent

with the observation that *Paramecium* RNAi factors are capable of processing both endogenously and exogenously derived mRNA[42,44]. The ability to facilitate a cost to host growth through delivery of single-stranded RNA, in the same orientation as the host target mRNA, therefore supports the hypothesis that a cost to host growth upon endosymbiont digestion can be facilitated by host RNAi-mediated RNA-RNA interactions between endosymbiont and host mRNA populations.

DISCUSSION

Through manipulation of the *P. bursaria* – *Chlorella* spp. endosymbiotic system, we have demonstrated that RNA released upon digestion of the algal endosymbiont is processed by the host RNAi system. For endosymbiont-derived mRNA sharing a high-level of sequence identity with host transcripts, this processing can result in knock-down of endogenous host gene expression, resulting in a cost to host growth (**Fig. S1**). We therefore postulate that these RNA-RNA interactions are of importance in eukaryote-eukaryote endosymbioses where partners are likely to share greater sequence similarity, especially among conserved transcripts which tend to be more highly represented among lethal or conditionally essential genes[56]. Due to the inherent difficulty in characterising such mechanisms directly, we have relied on a multiple experimental approach to demonstrate the viability of putative RNA-RNA interactions at each stage of the process. We have tracked the interaction through sRNA sequencing, recapitulated the effect through exposure to synthetic endosymbiont-derived RNA – including sense ssRNA analogous to endosymbiont mRNA – and demonstrated that this mechanism is mediated by host Dicer, Piwi, Pds1 and RdRP proteins. This process of host gene knock-down in response to endosymbiont-derived RNA processing by host RNAi factors, which we term 'RNAi-collisions', represents a candidate enforcement mechanism to sanction the host for breakdown of the interaction, a factor that would promote stability in a nascent eukaryote-eukaryote endosymbiosis.

The long-term maintenance of symbiotic interactions represents a quandary for evolutionary theory[30–35]. How do such relationships avoid over-exploitation by one partner that would ultimately lead the interaction to collapse? Partner switching is one option, however the result is typically a reduced pattern of co-evolution between symbiont and host that can inhibit the process of metabolic and genetic integration, stalling the evolution of stable interactions which are needed if a system is to move towards evolution of an

organelle[13,57–60]. Previous studies have suggested that when selfish behaviours arise, the evolution of enforcement to punish or suppress the exploitative partner can act to restore cooperation[9,10]. Enforcement mechanisms have been identified in diverse biological systems[61,62], and are argued to be one of the most effective drivers of cooperation in egalitarian alliances between different species, such as that between *P. bursaria* and its algal endosymbiont[9]. The results presented here suggest that 'RNAi collisions' between endosymbiont and host, which are capable of imposing a cost to host growth for breakdown of the symbiosis, could provide an emergent enforcement mechanism to discourage over-exploitation of the endosymbiont population by the host.

Interestingly, the emergence of this mechanism appears to be a by-product of pre-existing biological features that are already likely to be under strong selective pressure. For instance, the widely functional RNAi system of the host[42,43,45], or the conserved gene repertoire and sequence composition of the host and endosymbiont transcriptomes from which some 'RNAi collisions' have here been identified (including many transcripts which are conditionally essential in other systems[56]). Unlike comparable mechanisms of RNA-RNA interactions that have been studied in host-pathogen symbioses[36–40], these 'RNAi collisions' appear to be untargeted and, hence, emergent. In the aforementioned host-pathogen systems, targeted RNA is passed from one partner to the other in order to modulate expression of transcripts involved in virulence or resistance[36,39,40]. However, in order for such systems to evolve, they must first exist in an untargeted form upon which selection is able to act, allowing the emergence of specific RNA factors[37,38]. Identification of undirected 'RNAi collisions' in the *P. bursaria* – *Chlorella* system represents one such intermediary state, emergent in nature and untargeted, upon which sustained cellular interaction coupled with the potential for host-symbiont conflict could drive the selection of targeted RNA-RNA interactions.

We therefore propose that 'RNAi collisions' represent a putative mechanism to discourage over-exploitation of the endosymbiont population by the host. Here we have used the example of mass endosymbiont digestion in response to drug treatment to simulate this effect in the extreme. In natural interactions between *P. bursaria* and its algal endosymbiont, such a cost would only need to occur in the drastic occurrence of mass endosymbiont digestion in order to drive stability of the interaction. Importantly, the

403 endosymbiotic algal population within *P. bursaria* is largely composed of closely related or
404 clonal lineages[11–13], and as such, the fate of the algal population should be considered as a
405 collective unit. This cost need only act to supress large-scale, rapid destruction by the host in
406 order to drive the maintenance of a surviving subsection of the endosymbiont population.
407 Previous studies have demonstrated how *P. bursaria* is capable of manipulating
408 endosymbiont load in response to varying light conditions to better suit its own ends[27,28],
409 however, in these examples, reduction of endosymbiont number through digestion is slow
410 and partial. By providing a system that selects against rapid and near-complete digestion of
411 the endosymbiont population, 'RNAi collisions' effectively buffer the nascent endosymbiotic
412 interaction against total breakdown. We suggest that this has allowed the relationship to be
413 maintained across time and varying ecological conditions, even in the event of host-
414 symbiont conflict[27,28] and fluctuating endosymbiont numbers[14,26,27]. As an alternate route to
415 conflict resolution that avoids partner switching, we propose that such a mechanism would
416 facilitate greater co-evolution between endosymbiont and host. Over time, this would allow
417 the metabolic and genetic integration that drives the formation of obligate symbioses to
418 become manifest. We therefore present 'RNAi collisions' as a new mechanism in this
419 endosymbiotic system – a factor which can promote stability in the face of conflict in an
420 emergent endosymbiotic eukaryote-eukaryote cell-cell interaction.

421 **AUTHOR CONTRIBUTIONS**

422 B.H.J., D.S.M., and T.A.R. conceived and designed the experiments. F.M. and T.A.R.
423 conceived and designed the eDicer computational analysis. B.H.J., D.S.M., and T.A.R. wrote
424 the manuscript. B.H.J., D.S.M., F.M. and G.L. conducted experimental work and analysed the
425 data. B.E.H., S.W. and J.D.E aided in conceptual and experimental design, and in conducting
426 experimental work.

427 **ACKNOWLEDGEMENTS**

428 This work was primarily supported by an EMBO YIP award and a Royal Society University
429 Research Fellowship (UF130382) and latterly by an ERC Consolidator Grant (CELL-in-CELL) to
430 T.A.R. S.W. and J.D.E. were supported by awards from the Wellcome Trust
431 (WT107791/Z/15/Z) and the Lister institute. F.M. was supported by a Donald Hill Family
432 Fellowship in Computer Science. We thank Karen Moore and the University of Exeter
433 Sequence Service for support with the various sequencing projects. We thank Éric Meyer,

Institut de Biologie de l'Ecole Normale Supérieure, Paris, for advice during set up of the *P. bursaria* RNAi approach.

DECLARATION OF INTERESTS

The authors declare no competing interests.

FIGURES

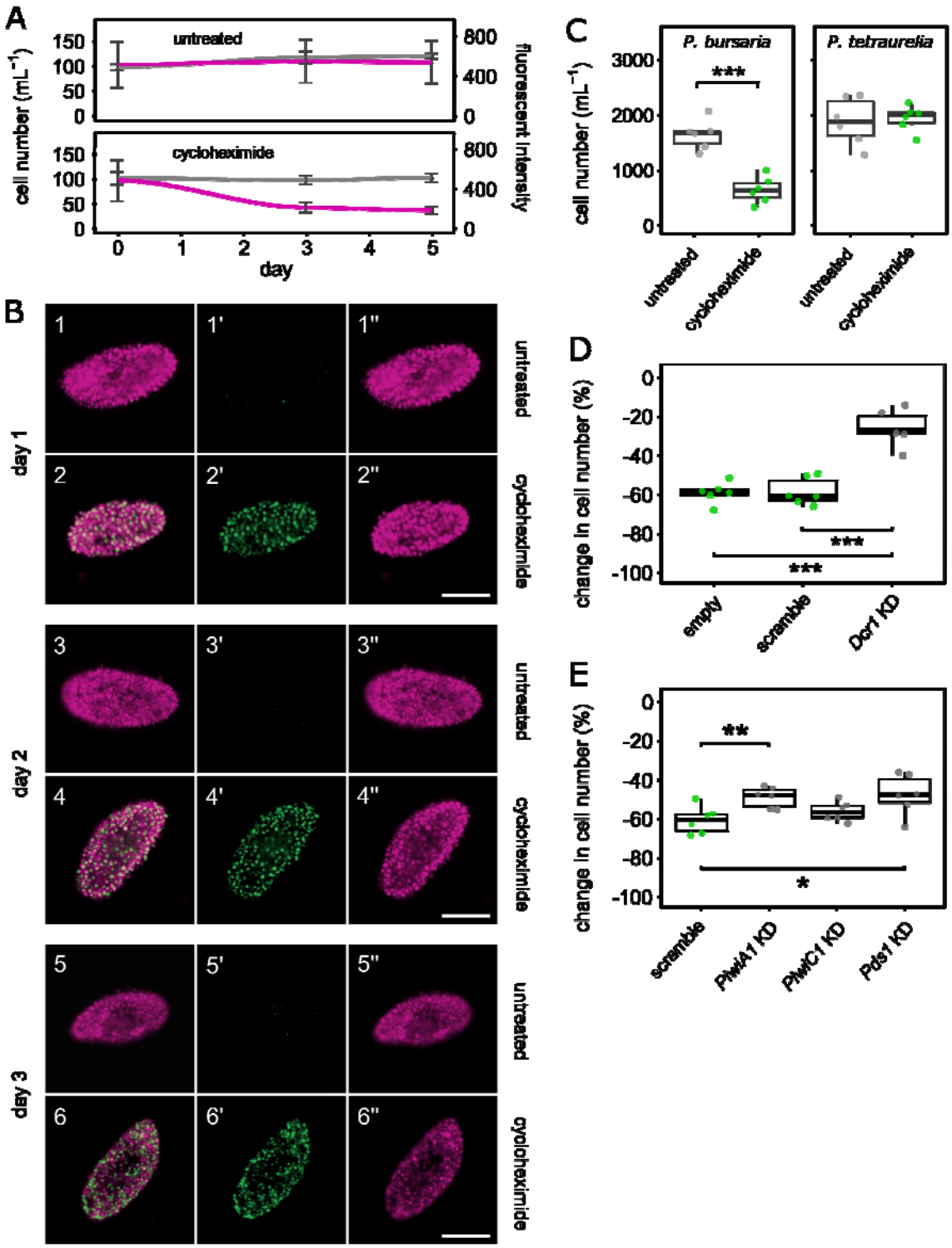
A
untreated
cycloheximide
cell number (mL⁻¹)
fluorescent intensity
day
B
day 1
day 2
day 3
untreated
cycloheximide
C
P. bursaria
P. tetraurelia
cell number (mL⁻¹)
***
D
change in cell number (%)
empty
scramble
Dcr1 KD
E
**
*
PwiA1 KD
PwiC1 KD
Pds1 KD

441 **Figure 1. Endosymbiont digestion in *P. bursaria* results in an RNAi-mediated 'physiological**
442 **cost' to the host.** (**A**) *Paramecium* cell number (grey) vs algal chlorophyll fluorescent
443 intensity (pink) in stationary phase *P. bursaria* cultures treated with cycloheximide (50
444 μgmL^{-1}), compared to untreated controls. Loss of algal fluorescent intensity indicates algal
445 death in response to cycloheximide treatment. Data are represented as mean ± SD of six
446 biological replicates. (**B**) Stages of endosymbiont elimination in *P. bursaria* cells over three
447 days of cycloheximide treatment (50 μgmL^{-1}). Algal chlorophyll fluorescence (pink) highlights
448 endosymbiotic algae within the *P. bursaria* cell. LysoTracker Green fluorescence (green)
449 indicates increased host lysosomal activity in response to cycloheximide treatment. Scale
450 bar – 50 µm. (**C**) *Paramecium* cell number in *P. bursaria* or *P. tetraurelia* cultures after 8 days
451 of treatment with cycloheximide (50 μgmL^{-1}; green), compared to untreated controls (light
452 grey). *Paramecium* cultures were fed with *E. coli* transformed with an empty RNAi vector.
453 (**D**) Percentage change in *P. bursaria* cell number in cultures treated with cycloheximide (50
454 μgmL^{-1}), compared to untreated controls, after 12 days of feeding with *E. coli* expressing;
455 Dicer (*Dcr1*) dsRNA (dark grey) to induce knock-down (KD), non-hit 'scramble' dsRNA or an
456 empty vector control (green). The relative effect of Dicer dsRNA exposure indicates partial
457 rescue of *P. bursaria* culture growth retardation in response to cycloheximide induced
458 endosymbiont digestion. (**E**) Percentage change in *P. bursaria* cell number in cultures
459 treated with cycloheximide (50 μgmL^{-1}), compared to untreated controls, after 12 days of
460 feeding with *E. coli* expressing; *PiwiA1, PiwiC1* or *Pds1* dsRNA (dark grey) to induce knock-
461 down (KD), or a non-hit 'scramble' dsRNA control (green). (**C-E**) Feeding was conducted daily
462 for four days prior to cycloheximide treatment, and continued throughout. Boxplot data are
463 represented as max, upper quartile (Q3), mean, lower quartile (Q1) and min values of six
464 biological replicates. Individual data points are shown. Significance calculated as $*p \leq 0.05$,
465 $**p \leq 0.01$, and $***p \leq 0.001$, using a generalized linear model with quasi-Poisson
466 distribution. See also **Figure S3** for the raw count data used to calculate the percentage
467 change in cell number presented in **1D-E**.

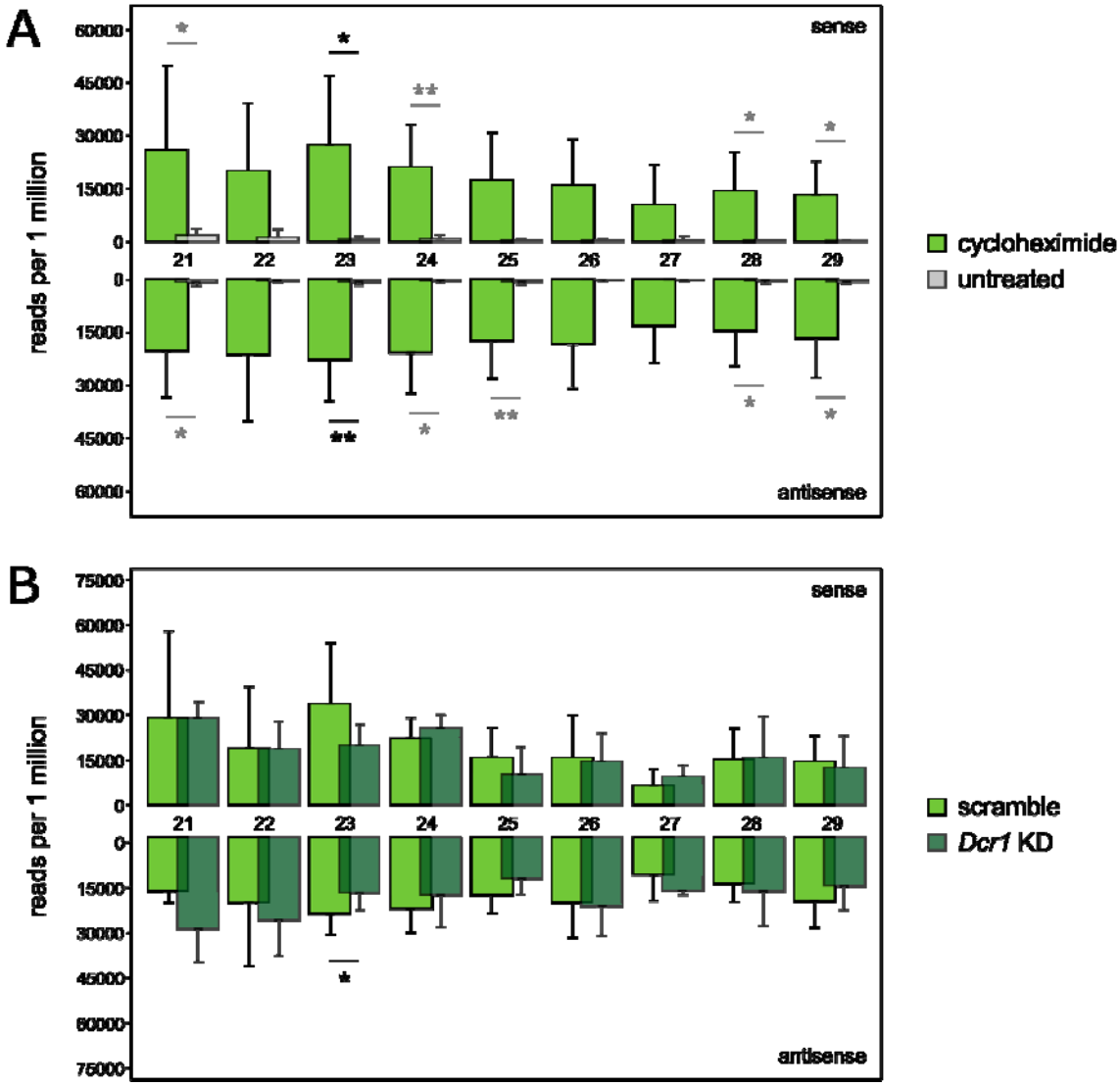

468

469

470 **Figure 2. Endosymbiont breakdown triggers an influx of Dicer-dependent endosymbiont-**
471 **derived sRNA within *P. bursaria*. (A)** Size distribution (nt) of sRNA mapped to
472 endosymbiont-derived cytoplasmic mRNA. sRNA was extracted from *P. bursaria* cultures
473 over two days (day 2 and 3) of cycloheximide treatment (50 μgmL^{-1}), or from untreated
474 controls. Note the relative increase in 23-nt abundance between untreated and
475 cycloheximide treated cultures. *P. bursaria* cultures were fed with *E. coli* transformed to
476 express non-hit 'scramble' dsRNA. Data are represented as mean ± SD of six biological
477 replicates, and normalised against total endosymbiont mRNA-mapping 21-29-nt reads per
478 dataset. (**B**) Size distribution (nt) of sRNA mapped to endosymbiont-derived cytoplasmic
479 mRNA. sRNA was extracted from *P. bursaria* cultures on day 3 of cycloheximide treatment

480 (50 µgmL^{-1}). *P. bursaria* cultures were fed with *E. coli* transformed to express Dicer (*Dcr1*)
481 dsRNA to induce knock-down (KD), or a non-hit 'scramble' dsRNA control. Note the relative
482 increase in 23-nt abundance during cycloheximide treatment in *P. bursaria* cultures exposed
483 to scramble dsRNA, compared to Dicer dsRNA. Data are represented as mean ± SD of three
484 biological replicates, and normalised against total endosymbiont mRNA-mapping 21-29-nt
485 reads per dataset. (**A**-**B**) Feeding was conducted daily for four days prior to cycloheximide
486 treatment, and continued throughout. Significance calculated as *$p \leq 0.05$, **$p \leq 0.01$, and
487 ***$p \leq 0.001$ using a generalised linear model with quasi-Poisson distribution. All curated
488 'endosymbiont' mRNA transcript bins used for sRNA mapping are available on Figshare
489 (10.6084/m9.figshare.12301736). See also **Figure S4** for sRNA abundance at each individual
490 day.

491

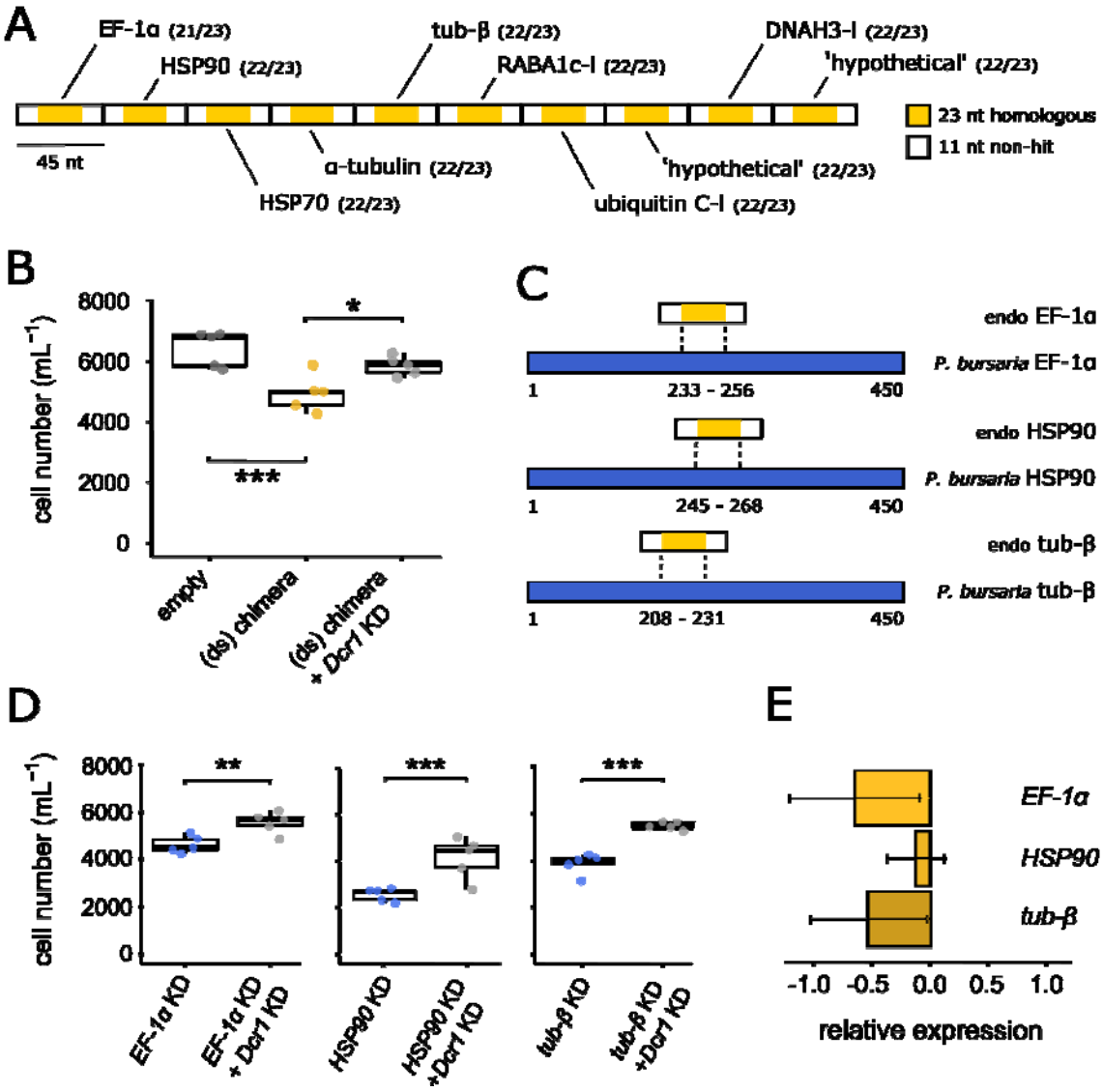

Figure 3. ***In vivo*** **exposure to a synthetic endosymbiont-derived RNA chimera generates simultaneous knock-down of homologous host genes in** ***P. bursaria*****.** (**A**) Schematic showing chimeric construct design. Ten endosymbiont-derived 45-nt transcript sequences (**Table S3**), featuring a 23-nt region with >91% sequence identity between endosymbiont and host (yellow) flanked by 11-nt of 'non-hit' algal transcript (white). Numbers in brackets denote sequence identity between endosymbiont and host. (**B**) *P. bursaria* cell number after 12 days of feeding with *E. coli* expressing: chimera dsRNA (yellow); chimera dsRNA mixed with Dicer (*Dcr1*) dsRNA (light grey; rescue); or an empty vector control (dark grey). See **Figure S9** for an experimental dilution of dsRNA chimera delivery. (**C**) Schematic demonstrating the

503 degree of overlap between three endosymbiont (endo) derived transcripts from the
504 chimeric construct (white/yellow) and respective 450-nt homologous region of the host (*P.*
505 *bursaria*) transcript (blue). Each region of 23-nt overlap (yellow) represents putative RNAi
506 'collisions' between endosymbiont and host. (**D**) *P. bursaria* cell number after 12 days of
507 feeding with *E. coli* expressing: host *EF1-α*, *HSP90* or *tub-β* 450-nt dsRNA (blue) to induce
508 host knock-down (KD), compared to Dicer (*Dcr1*) dsRNA mixed controls (grey; rescue
509 phenotype). See also **Figure S11** for individual knock-down (KD) of each of the ten broader
510 host targets of the endosymbiont-derived dsRNA chimera. (**E**) qPCR of mRNA extracted from
511 day 3 of chimera-RNAi feeding (**3B**), revealing knock-down of *EF1-α*, *HSP90* and *tub-β* host
512 gene expression in *P. bursaria* in response to endosymbiont derived chimera dsRNA
513 exposure. Standardised expression of an Actin housekeeping gene was used for
514 normalisation. Data are represented as mean ± SD of three biological replicates. These three
515 genes were assessed for knock-down as a result of endosymbiont derived chimera
516 exposure, based on evidence that directed knock-down of the wider corresponding host
517 gene led to retardation of *P. bursaria* culture growth (**3D**). For an extended figure showing
518 the effect of Dicer knock-down on the expression of these three host genes, see **Figure S12**.
519 (**B**/**D**) Multiple vector delivery was conducted at a 50:50 ratio during feeding. Boxplot data
520 are represented as max, upper quartile (Q3), mean, lower quartile (Q1) and min values of
521 five biological replicates. Individual data points are shown. Significance for boxplot data
522 calculated as $*p \leq 0.05$, $**p \leq 0.01$, $***p \leq 0.001$, using a generalized linear model with
523 quasi-Poisson distribution.

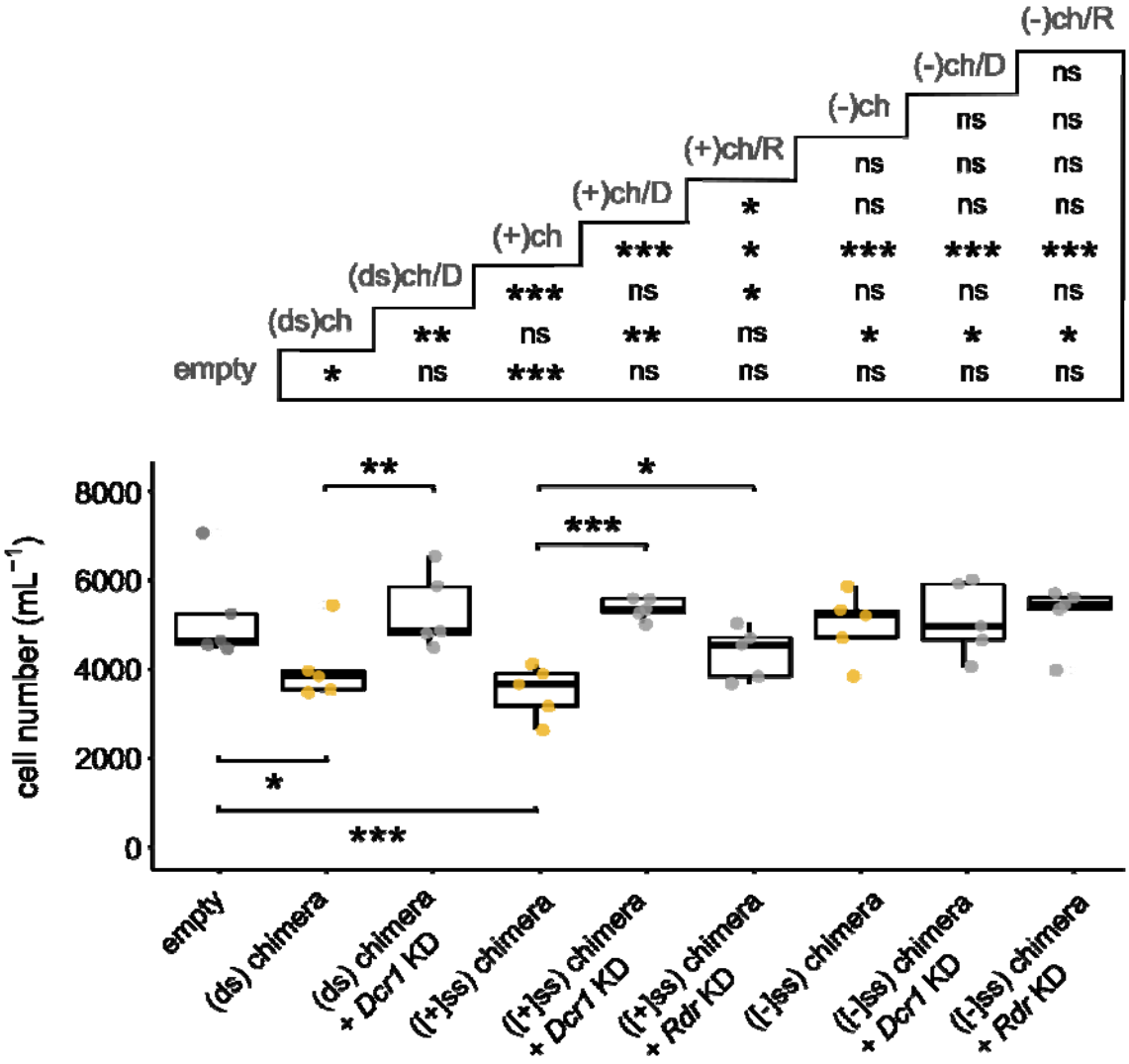

Figure 4. Single-stranded delivery of synthetic endosymbiont-derived RNA, analogous to endosymbiont mRNA, results in a cost to *P. bursaria* growth. *P. bursaria* cell number after 14 days of feeding with *E. coli* expressing; chimera RNA in ds, [+]ss or [-]ss orientation (yellow); chimera RNA in ds, [+]ss or [-]ss orientation mixed with Dicer (*Dcr1*) or RdRP (*Rdr*) dsRNA (light grey; rescue); or an empty vector control (dark grey). Multiple vector delivery was conducted at a 50:50 ratio during feeding. Asterisks displayed in the grid above denote pairwise significance values. Boxplot data are represented as max, upper quartile (Q3), mean, lower quartile (Q1) and min values of five biological replicates. All significance for boxplot data calculated as *p ≤ 0.05, **p ≤ 0.01, ***p ≤ 0.001, 'ns' no significance, using a generalized linear model with quasi-Poisson distribution.

536 **METHODS**

537 ***Culture conditions and media***

538 In all RNAi experiments, *Paramecium bursaria* 186b (CCAP 1660/18) strain was used. For
539 experiments requiring a non-photo-endosymbiotic *Paramecium* system for comparison,
540 *Paramecium tetraurelia* nd7 strain was used. For eDicer analysis, *Paramecium bursaria* 186b
541 and Yad1g1N strains were used[41,55].

542 *Paramecium* cells were cultured in New Cereal Leaf – Prescott Liquid media (NCL). NCL
543 media was prepared by adding 4.3 mgL^{-1} $CaCl_2.2H_2O$, 1.6 mgL^{-1} KCl, 5.1 mgL^{-1} K_2HPO_4, 2.8
544 mgL^{-1} $MgSO_4.7H_2O$ to deionised water. 1 gL^{-1} wheat bran was added, and the solution boiled
545 for 5 minutes. Once cooled, media was filtered once through Whatman Grade 1 filter paper
546 and then through Whatman GF/C glass microfiber filter paper. Filtered NCL media was
547 autoclaved at 121°C for 30 mins to sterilise prior to use.

548 NCL medium was bacterized with *Klebsiella pneumoniae* SMC and supplemented with
549 0.8 mgL^{-1} β-sitosterol prior to propagation. *Paramecium* cells were sub-cultured 1:9 into
550 fresh bacterized NCL media once per month for *Paramecium bursaria* 186b, and once every
551 two weeks for *Paramecium tetraurelia* nd7. *Paramecium* cultures were maintained at 18°C
552 with a light-dark (LD) cycle of 12:12h.

553 ***LysoTracker staining and fluorescent imaging***

554 *Paramecium* cells were fixed using 0.5% paraformaldehyde and incubated for 20 mins at RT.
555 Cells were then treated with 2 µM LysoTracker Green DND-26 (Invitrogen) to stain acidic
556 vesicles such as the lysosome, and incubated in constant darkness for 2 hours at RT prior to
557 imaging. Stained *Paramecium* cells were imaged on an ImageXpress Pico Automated Cell
558 Imaging System at 10x magnification, using the Cy5 (absorbance – 630/40 nm, emission –
559 695/45 nm) and FITC (absorbance – 465/40 nm, emission – 525/30 nm) channels to capture
560 algal chlorophyll autofluorescence and LysoTracker Green DND-26 fluorescence
561 respectively.

562 ***Gene synthesis and construct design***

563 Sequences for plasmid constructs were synthesised *de novo* by either Genscript or SynBio
564 Technologies, and cloned into an L4440 plasmid vector. Sequences and cloning sites for

565 each plasmid construct are detailed in **Table S1**. All modified constructs were confirmed by
566 Sanger sequencing (Eurofins Genomics).

567 ***RNAi feeding***

568 *Paramecium* was fed with *E. coli* transformed with an L4440 plasmid construct with paired
569 IPTG-inducible T7 promoters, facilitating targeted gene knock-down through the delivery of
570 complementary double-stranded RNA (dsRNA). L4440 plasmid constructs were transformed
571 into *E. coli* HT115 competent cells and grown overnight on LB agar (50 μgmL^{-1} Ampicillin and
572 12.5 μgmL^{-1} Tetracycline) at 37°C. Positive transformants were picked and grown overnight
573 in LB (50 μgmL^{-1} Ampicillin and 12.5 μgmL^{-1} Tetracycline) at 37°C with shaking (180 rpm).
574 Overnight pre-cultures were back-diluted 1:25 into 50 mL of LB (50 μgmL^{-1} Ampicillin and
575 12.5 μgmL^{-1} Tetracycline) and incubated for a further 2 hours under the same conditions,
576 until an OD_{600} of between 0.4 and 0.6 was reached. *E. coli* cultures were then supplemented
577 with 0.4 mM IPTG to induce template expression within the L4440 plasmid, and incubated
578 for a further 3 hours under the same conditions. *E. coli* cells were pelleted by centrifugation
579 (3100 x *g* for 2 mins), washed with sterile NCL media, and pelleted once more. *E. coli* cells
580 were then re-suspended in NCL media supplemented with 0.4 mM IPTG, 100 μgmL^{-1}
581 Ampicillin, and 0.8 μgmL^{-1} β-sitosterol, and adjusted to a final OD_{600} of 0.1.

582 *Paramecium* cells were pelleted by gentle centrifugation in a 96-well plate (10 mins
583 at 800 x *g*), taking care not to disturb the cell pellet by leaving 50 µl of supernatant, and re-
584 suspended 1:4 into 200 µl of induced *E. coli* culture media (to make 250 µl total). Feeding
585 was conducted daily for up to 14 days using freshly prepared bacterized media.

586 ***Single-stranded construct design and confirmation***

587 To create a version of L4440 which expressed only single-stranded (ssRNA), L4440 was
588 digested with KpnI and PvuII (Promega), gel-purified (Wizard SV Gel and PCR Clean-Up
589 System, Promega) and blunted using *PfuUltra* HF DNA polymerase (Agilent Technologies).
590 The blunt vector was re-ligated using T4 DNA ligase (Thermo Scientific) and confirmed by
591 sequencing (Eurofins Genomics), generating plasmid pDM004 which contains only a single
592 T7 promoter. Fragments were then excised from their respective L4440 plasmids, or
593 amplified by PCR (Q5 Polymerase; New England Biolabs) to swap the restriction sites,
594 digested, and ligated into pDM004 to generate plasmids containing inserted fragments in

595 sense [+] or antisense [-] orientation. Generated plasmids were transformed into HT115 *E.*
596 *coli* for use in RNAi feeding experiments.

597 To confirm that these plasmid constructs generated only ssRNA, cultures of *E. coli*
598 HT115 containing pDM005-1 ([-]ssRNA chimera) or pDM005-2 ([+]ssRNA chimera) were
599 grown overnight at 37°C, 180 rpm in LB supplemented with 50 μgmL^{-1} ampicillin and 12.5
600 μgmL^{-1} tetracycline. Cultures were diluted 1:25 in fresh medium and grown to an OD_{600} of
601 0.4-0.6. Expression was then induced with 400 µM IPTG for 3 hrs, after which 1 mL of
602 culture was pelleted by centrifugation for 2 mins at 3,100 x *g*. RNA was extracted using an
603 RNeasy Mini Kit (Qiagen), following the manufacturer's protocol for Total RNA Purification
604 from Animal Cells. 20 µl of RNA was then treated with 10 μgmL^{-1} RNase A (Sigma-Aldrich) for
605 1 hour at 30°C in the presence of 300 mM NaCl (stabilising dsRNA and allowing RNase A to
606 degrade only ssRNA[63]). A separate aliquot was left untreated, with 300 mM NaCl added to
607 facilitate precipitation. All samples were then extracted with 1:1 phenol:chloroform and
608 precipitated with 2 volumes of ethanol. Pellets were washed twice with 80% ethanol and re-
609 suspended in nuclease-free water. RNA samples were then cleared of residual genomic DNA
610 using the TURBO DNA-*free* Kit (Ambion), following the manufacturer's protocol for routine
611 DNase treatment. RT-PCR was then performed using the Qiagen OneStep RT-PCR kit
612 following the manufacturer's instructions, with 0.5 µL template RNA and 0.6 µM each
613 primer (pDM005_RT_F: 5'-ACTTCAATGATTCGCAGCGG-3' and pDM005_RT_R: 5'-
614 AAGTAGCTGCTGTTCTCGGT-3'), generating an 85-nt PCR product. Cycling conditions were as
615 detailed in the manufacturer's protocol (30 cycles), with 1 min annealing at 50°C. PCR
616 products were then resolved on a 2% agarose gel to assess for the presence/absence of
617 amplification in each sample (**Figure S11**).

618 ***qPCR analysis***

619 RNA was extracted from *P. bursaria* 186b for gene expression analysis after three days of
620 RNAi feeding. *Paramecium* cells (~10^3 per culture) were pelleted by gentle centrifugation
621 (800 x *g* for 10 mins), snap-frozen in liquid nitrogen, and stored at -80°C. RNA extraction was
622 performed using TRIzol reagent (Invitrogen), following the manufacturer's protocol after re-
623 suspending each pellet in 900 µl TRIzol reagent. RNA was precipitated using GlycoBlue Co-
624 precipitant (Invitrogen) to aid RNA pellet visualisation, and then cleared of residual DNA

625 using the TURBO DNA-*free* Kit (Ambion), following the manufacturer's protocol for routine
626 DNase treatment.

627 RNA was reverse transcribed into single stranded cDNA using the SuperScript® III First-
628 Strand Synthesis SuperMix (Invitrogen), following the manufacturer's protocol. Quantitative
629 PCR (qPCR) was performed in a StepOnePlus Real-Time PCR system (Thermo Fisher
630 Scientific). Reaction conditions were optimised using a gradient PCR, with a standard curve
631 determined using 10-fold dilutions of *P. bursaria* cDNA: *EF-1α* (slope: -3.353; R^2: 0.999;
632 efficiency 98.740%), *HSP90* (slope: -3.319; R2: 0.998; efficiency 100.131%), *tub-β* (slope: -
633 3.378; R^2: 0.992; efficiency 97.692%), and *actin* (slope: -3.349; R^2: 0.983; efficiency
634 98.866%), using StepOne software v2.3. Each 20 µL reaction contained 10 µL PowerUp SYBR
635 Green Master Mix (Thermo Fisher Scientific), 500 nM each primer (300 nM for *tub-β*) and 1
636 µL (50 ng) cDNA. Each reaction was performed in duplicate for each of 3 biological
637 replicates, alongside a 'no-RT' (i.e. non-reverse transcribed RNA) control to detect any
638 genomic DNA contamination. Cycling conditions were as follows: UDG activation, 2 mins at
639 50°C and DNA polymerase activation, 2 mins at 95°C, followed by 40 cycles of 15 secs, 95°C
640 and 1 min at 55-65°C (*EF-1α* (58°C), *HSP90* (58°C), *tub-β* (57°C) and *actin* (58°C)). Primers
641 pairs for each reaction are listed in **Table S5**. Each reaction was followed by melt-curve
642 analysis, with a 60-95°C temperature gradient (0.3°C s^{-1}), ensuring the presence of only a
643 single amplicon, and ROX was used as a reference dye for calculation of C_T values. C_T values
644 were then used to calculate the change in gene expression of the target gene in RNAi
645 samples relative to control samples, using a derivation of the $2^{-\Delta\Delta CT}$ algorithm[64].

646 ***sRNA isolation and sequencing***

647 Total RNA for sRNA sequencing was extracted from *P. bursaria* (or free-living algal) cultures
648 using TRIzol reagent (Invitrogen), as detailed above. To isolate sRNA from total RNA,
649 samples were size separated on a denaturing 15% TBE-UREA polyacrylamide gel. Gels were
650 prepared with a 15 mL mix with final concentrations of 15% Acrylamide/Bis (19:1), 8M
651 UREA, TBE (89 mM Tris, 89 mM Borate, 2 mM EDTA), and the polymerisation started by the
652 addition of 150 µL 10% APS (Sigma-Aldrich) and 20 µL TEMED (Sigma-Aldrich). Gels were
653 pre-equilibrated by running for 15 mins (200 V, 30 mA) in TBE before RNA loading. The
654 ladder mix consisted of 500 ng ssRNA ladder (50-1000nt, NEB#N0364S), and 5-10 ng of each
655 21 & 26-nt RNA oligo loaded per lane. The marker and samples were mixed with 2X RNA

656 loading dye (NEB) and heat denatured at 90 °C for 3 mins before snap cooling on ice for 2
657 min prior to loading. Blank lanes were left between samples/replicates to prevent cross-
658 contamination during band excision. Gels were then run for 50 mins (200V, 30 mA).

659 Once run, gels were stained by shaking (60 rpm) for 20 mins at RT in a 40 mL TBE
660 solution containing 4 µL SYBR® Gold Nucleic Acid Gel Stain. Bands of the desired size range
661 (~15-30 nt) were visualised under blue light, excised and placed into a 0.5 mL tube pierced
662 at the bottom by a 21-gauge needle, resting within a 1.5 mL tube, and centrifuged (16,000 x
663 *g* for 1 min). 400 µL of RNA elution buffer (1M Sodium acetate pH 5.5 and 1mM EDTA) was
664 added to the 1.5 mL tube containing centrifuged gel slurry, and the empty 0.5 mL tube
665 discarded. Gel slurry was manually homogenized until dissolved using a 1 mL sterile plunger
666 and incubated at RT for 2 hours with shaking at 1,400 rpm.

667 Solutions containing RNA elution buffer and gel slurry were transferred to a Costar
668 Spin-X 0.22 µm filter column and centrifuged (16,000 x *g* for 1 min). The filter insert
669 containing acrylamide was discarded. 1 mL of 100% EtOH was added to each solution,
670 alongside 15 µg of GlycoBlue™ Coprecipitant (Invitrogen) to aid sRNA pellet visualisation,
671 and stored overnight at -80°C to precipitate. Precipitated solutions were centrifuged at 4°C
672 (12,000 x *g* for 30 mins), and the supernatant discarded. sRNA pellets were washed with 500
673 µL of cold 70% EtOH (12,000 x *g* for 15 mins at 4°C), and air dried in a sterile PCR hood for
674 10 mins, before re-suspending in 15 µL of RNAse-free water and storage at -80°C.

675 ***sRNA-seq and read processing***

676 sRNA concentrations were determined using an Agilent 2100 Bioanalyzer, following the
677 Agilent Small RNA kit protocol, and all samples matched to 0.7 $ngmL^{-1}$ prior to sequencing.
678 Library preparation and subsequent RNA-seq was performed for 54 samples using 50-bp
679 paired-end, rapid run across four lanes on an Illumina HiSeq 2500, yielding ~120-150 million
680 paired-end reads per lane (~9-11 million paired-end reads per sample).

681 The raw paired-end reads from the RNA-seq libraries were trimmed using Trim Galore
682 in order to remove barcodes (4-nt from each 3'- and 5'- end) and sRNA adaptors, with
683 additional settings of a phred-score quality threshold of 20 and minimum length of 16-nt.
684 Result were subsequently checked with FastQC.

685 ***Assigning sRNAs to the algal endosymbiont transcript bins***

686 Trimmed reads were mapped against the 'endosymbiont' dataset of assembled transcripts
687 using the HISAT2 alignment program with default settings. Post-mapping, the BAM files
688 were processed using SAMTOOLS and a set of custom scripts
689 (https://github.com/guyleonard/paramecium) to produce a table of mapped read
690 accessions and their respective read lengths. Using these exported count tables, of mapped
691 reads per read length, transcripts with >10 hits for read lengths between 21-25 nt were
692 searched using reciprocal BLASTX against the NCBI non-redundant 'nr' proteins sequence
693 database, in order to assign taxonomic identity to each transcript. This allowed filtering of
694 the main 'endosymbiont' dataset into subsets corresponding to either: algal cytoplasmic
695 mRNA, algal cytoplasmic rRNA, algal plastid RNA or algal mitochondrial RNA; host RNA
696 contamination; bacterial RNA contamination; or vector RNA contamination. All identified
697 algal cytoplasmic rRNA (28 transcripts), plastid RNA (56 transcripts) or mitochondrial RNA
698 (18 transcripts) sequences were sorted into new datasets representing each RNA species.
699 Host (5 transcripts) and bacterial (34 transcripts) contamination were sorted into respective
700 'host' or 'bacterial' datasets. Vector (1 transcript) and all unidentifiable sequences (20
701 transcripts) were separated into a dataset labelled as 'other'. All remaining transcripts with
702 >10 sRNA hits for read sizes 21-25 nt in the original dataset now represented putative algal
703 mRNA transcripts (i.e. for 23-nt reads this represented 3,659 sRNA reads mapping to 148
704 transcripts). In this algal mRNA dataset, we also included transcripts that fell below the >10
705 sRNA hit threshold for manual curation, and which therefore may correspond to reads
706 mapping to all of the above bins (i.e. for 23-nt reads this represented 1,949 reads mapping
707 to 605 transcripts in total, of which 1,408 reads were mapping to 468 transcripts which were
708 not manually curated, so could be affected by contamination). This manual binning process
709 was carried out in order to double check the original automated binning post transcriptome
710 assembly, and to check for possible chimeric host-algal transcript sequences produced as a
711 by-product of cDNA synthesis and transcriptome sequencing and assembly. This process
712 collectively allowed accurate segregation of the existing 'endosymbiont' transcript bin into
713 discrete subsets based on RNA 'species'.

714 Using the HISAT2 alignment program with default settings, trimmed reads were
715 mapped once more against the newly filtered algal mRNA, rRNA, plastid and mitochondrial
716 datasets from above. Count tables of mapped reads per read length were once again

717 generated from the BAM files, and used to plot a size distribution of 21-29 nt endosymbiont
718 derived sRNA abundance per RNA species. Size distributions of sRNA abundance for each
719 sample were plotted using the R programming language packages; tidyverse, grid.extra and
720 ggplot2 in R Studio.

721 ***eDicer methods for identifying putative RNA-RNA interactions***

722 To predict putative mRNA-mRNA interactions using eDicer
723 (https://github.com/fmaguire/eDicer), both the 'host' and 'endosymbiont' transcript bins
724 processed from transcriptome data for *P. bursaria* Yad1g1N[55] were further filtered to
725 minimise the risk of false positives for host and endosymbiont cross-comparisons. For the
726 'host' bins, any transcript with >90% ID BLASTN hit to the following genome assemblies
727 were removed: *Chlamydomonas reinhardtii* cc503 cw92 mt, *Chlamydomonas reinhardtii* v3,
728 *Chlorella sorokiniana* 1228 v2, *Chlorella sorokiniana* DOE1412 v3, or *Chlorella sorokiniana*
729 utex1230 lanl v2 assemblies from Los Alamos National Labs Greenhouse genome database.
730 Similarly, for the 'endosymbiont' bins, any transcript with >90% ID BLASTN hit to the
731 following ParameciumDB genome assemblies were removed: *P. biaurelia* V1-4 v1, *P.*
732 *caudatum* 43c3d v1, *P. bursaria* MAC 110224 v1, *P. decaurelia* MAC 223 v1, *P. dodecaurelia*
733 MAC 274 v1, *P. jenningsi* MAC M v1, *P. novaurelia* MAC TE v1, *P. octaurelia* K8 CA1, *P.*
734 *quadecaurelia* MAC NiA v1, *P. primaurelia* Ir4-2 v1, *P. tetraurelia* MAC 51 with and without
735 IES, or *P. tetraurelia* MAC. Additionally, the reference (refseq) genome of *Escherichia coli*
736 MG1655 (NCBI acc.: NZ_CP012868.1) and *Klebsiella pneumoniae* HS11286 (NCBI acc.:
737 NC_016845.1) were used as 'food' comparison datasets.

738 The filtered 'endosymbiont' transcript bin, *E. coli* CDS and *K. pneumoniae* CDS were
739 decomposed into all possible 21-23 nt reads with jellyfish v2.2.10 and aligned with 95%
740 identity to the 'host' bin using Bowtie v1.2.3 (recommended for short alignments). These *in-*
741 silico RNA-RNA interaction simulations were performed using a wrapper tool we created
742 named eDicer (v1.0.0) (https://github.com/fmaguire/eDicer). The number of distinct
743 aligning k-mers (i.e. putative interactions of unique sequences) for each pair of bins were
744 then normalised by dividing by the total number of distinct k-mers in both bins, and x 100,
745 to calculate a Jaccard Index % (i.e. normalised set similarity).

746 To predict putative 'lethal' RNA-RNA interactions, a separate analysis was conducted
747 using a subset of each dataset that was putatively homologous to a yeast 'lethal' gene

748 database[56]. This 'lethal' dataset contained genes known to be conditionally essential in
749 *Saccharomyces cerevisiae*. These putative 'lethal' homologues for each dataset were
750 identified using a tBLASTx search of the yeast 'lethal' database[56] with a gathering threshold
751 set at 1e-10 with a minimum of 50% sequence identity. Once curated, each 'lethal' dataset
752 was subject to eDicer analysis as described above.

753 To predict putative rRNA-rRNA interactions using eDicer, a further analysis was
754 conducted using a dataset consisting of full-length ribosomal RNA (rRNA) clusters for
755 *Microactinium conductrix* [NCBI acc.: ASM224581v2][65], *K. pneumoniae* [NCBI acc.:
756 NC_016845.1][66], *E. coli* [NCBI acc.: NZ_CP012868.1], *P. bursaria* Yad1g1N[55] and *P. bursaria*
757 186b. Once again, each dataset was subject to eDicer analysis as described above. All *in-*
758 *silico* RNA-RNA interaction predictions were plotted using the R programming language
759 packages; tidyverse, grid.extra and ggplot2 in R Studio.

760 ***Manual curation of additional host transcript bins***

761 In order to identify host transcripts that could be impacted by putative RNA-RNA
762 interactions as a result of endosymbiont derived sRNA exposure, trimmed Illumina reads for
763 all sRNA sequencing samples were mapped to the 'endosymbiont mRNA' transcript dataset.
764 Resulting mapping files were filtered with custom scripts
765 (https://github.com/guyleonard/paramecium) producing tables of mapped hits with their
766 respective read lengths. Reads from all tables, of length 23-nt only, were then extracted with
767 SEQTK (resulting in 3,690 total). A BLASTn search of these 23-nt endosymbiont reads was
768 conducted against the 'host' transcript dataset, to identify host transcripts with ≥ 95%
769 identity over a 23-nt region. This resulted in three candidate host transcripts. These three
770 host transcripts were searched using BLASTx against the NCBI non-redundant 'nr' protein
771 database, resulting in one transcript with 100% sequence identity to both endosymbiont
772 and host HSP90. For the remaining two transcripts, SNPs present in the identified 23-nt
773 mapped sequence indicate that these are putative host sequences with 2-nt of mismatch
774 compared to the respective endosymbiont sequence, and were therefore unlikely to
775 represent a product of RNA-RNA interactions between endosymbiont and host as a result of
776 endosymbiont derived 23-nt sRNA exposure.

777 In order to identify host transcripts that could be classified as 'non-hit' transcripts (i.e.
778 host transcripts sharing a low level of sequence identity with algal transcripts over 23-nt

regions), the 'host' dataset was searched using an organism specific BLASTn (Chlorellaceae [NCBI: taxid35461]) against the NCBI nucleotide 'nr/nt' database with a minimum expectation of 1e-05. Any host transcripts sharing >20-nt sequence identity with algal transcripts over a 23-nt region were rejected. This process was repeated until a dataset of 20 'non-hit-algal' host transcripts were identified. These putative 'non-hit-algal' host transcripts were then searched using BLASTx against the NCBI non-redundant 'nr' protein database, to confirm that these 20 transcripts were derived from *Paramecium* and were not bacterial contamination.

DATA AND SOFTWARE AVAILABILITY

The raw reads generated during sRNA sequencing are available on the NCBI Sequence Read Archive (accessions: SAMN14932981, SAMN14932982). All other datasets are available on Figshare (https://doi.org/10.6084/m9.figshare.c.4978160.v1), under the relevant headings. Custom scripts for sRNA read processing (https://github.com/guyleonard/paramecium, https://doi.org/10.5281/zenodo.4638888) and eDicer comparative analysis (https://github.com/fmaguire/eDicer, https://doi.org/10.5281/zenodo.4659378) are available on GitHub and archived within the Zenodo repository.

BIBLIOGRAPHY

1. Archibald, J. M. Endosymbiosis and eukaryotic cell evolution. *Curr. Biol.* **25**, R911-921 (2015).
2. Baurain, D. *et al.* Phylogenomic evidence for separate acquisition of plastids in Cryptophytes, Haptophytes, and Stramenopiles. *Molecular biology and evolution* **27**, 1698–709 (2010).
3. Keeling, P. J. The number, speed, and impact of plastid endosymbioses in eukaryotic evolution. *Annual Review of Plant Biology* **64**, 583–607 (2013).
4. Archibald, J. M. The puzzle of plastid evolution. *Curr Biol* **19**, R81-8 (2009).
5. Howe, C. J., Barbrook, A. C., Nisbet, R. E. R., Lockhart, P. J. & Larkum, A. W. D. The origin of plastids. *Philos Trans R Soc Lond B Biol Sci* **363**, 2675–2685 (2008).

6. Timmis, J. N., Ayliffe, M. A., Huang, C. Y. & Martin, W. Endosymbiotic gene transfer: organelle genomes forge eukaryotic chromosomes. *Nat. Rev. Genet.* **5**, 123–135 (2004).
7. Gray, M. W. Mitochondrial evolution. *Cold Spring Harb Perspect Biol* **4**, (2012).
8. Moran, N. A. Symbiosis as an adaptive process and source of phenotypic complexity. *Proc. Natl. Acad. Sci. U.S.A.* **104 Suppl 1**, 8627–8633 (2007).
9. Ågren, J. A., Davies, N. G. & Foster, K. R. Enforcement is central to the evolution of cooperation. *Nat Ecol Evol* **3**, 1018–1029 (2019).
10. West, S. A., Kiers, E. T., Simms, E. L. & Denison, R. F. Sanctions and mutualism stability: why do rhizobia fix nitrogen? *Proceedings of the Royal Society of London. Series B: Biological Sciences* **269**, 685–694 (2002).
11. Achilles-Day, U. E. & Day, J. G. Isolation of clonal cultures of endosymbiotic green algae from their ciliate hosts. *J Microbiol Methods* **92**, 355–7 (2013).
12. Hoshina, R. & Kusuoka, Y. DNA Analysis of algal endosymbionts of ciliates reveals the state of algal integration and the surprising specificity of the symbiosis. *Protist* **167**, 174–184 (2016).
13. Zagata, P., Greczek-Stachura, M., Tarcz, S. & Rautian, M. The evolutionary relationships between endosymbiotic green algae of *Paramecium bursaria* syngens originating from different geographical locations. *Folia Biol (Krakow)* **64**, 47–54 (2016).
14. Kodama, Y. & Fujishima, M. Cycloheximide induces synchronous swelling of perialgal vacuoles enclosing symbiotic *Chlorella vulgaris* and digestion of the algae in the ciliate *Paramecium bursaria*. *Protist* **159**, 483–94 (2008).
15. Kodama, Y. & Fujishima, M. Symbiotic *Chlorella variabilis* incubated under constant dark conditions for 24 hours loses the ability to avoid digestion by host lysosomal enzymes in digestive vacuoles of host ciliate *Paramecium bursaria*. *FEMS Microbiol. Ecol.* **90**, 946–955 (2014).

16. Omura, G. *et al.* A bacteria-free monoxenic culture of *Paramecium bursaria*: its growth characteristics and the re-establishment of symbiosis with *Chlorella* in bacteria-free conditions. *Jpn J Protozool* **37**, (2004).
17. Tanaka, M. *et al.* Complete elimination of endosymbiotic algae from *Paramecium bursaria* and its confirmation by diagnostic PCR. *Acta Protozool* **41**, 255–261 (2002).
18. Brown, J. A. & Nielsen, P. J. Transfer of photosynthetically produced carbohydrate from endosymbiotic Chlorellae to *Paramecium bursaria*. *J. Protozool.* **21**, 569–570 (1974).
19. Esteban, G. F., Fenchel, T. & Finlay, B. J. Mixotrophy in ciliates. *Protist* **161**, 621–641 (2010).
20. Johnson, M. D. Acquired phototrophy in ciliates: a review of cellular interactions and structural adaptations. *J Eukaryot Microbiol* **58**, 185–95 (2011).
21. Kato, Y. & Imamura, N. Amino acid transport systems of Japanese *Paramecium* symbiont F36-ZK. *Symbiosis* **47**, 99–107 (2009).
22. Kato, Y. & Imamura, N. Effect of sugars on amino acid transport by symbiotic *Chlorella*. *Plant Physiol Biochem* **46**, 911–7 (2008).
23. Kawakami, H. & Kawakami, N. Behavior of a virus in a symbiotic system, *Paramecium bursaria*—Zoochlorella. *The Journal of Protozoology* **25**, 217–225 (1978).
24. Parker, R. C. Symbiosis in *Paramecium bursaria*. *Journal of Experimental Zoology* **46**, 1–12 (1926).
25. Ziesenisz, E., Reisser, W. & Wiessner, W. Evidence of de novo synthesis of maltose excreted by the endosymbiotic *Chlorella* from *Paramecium bursaria*. *Planta* **153**, 481–485 (1981).
26. Kodama, Y. & Fujishima, M. Infectivity of *Chlorella* species for the ciliate *Paramecium bursaria* is not based on sugar residues of their cell wall components, but on their ability

to localize beneath the host cell membrane after escaping from the host digestive vacuole in the early infection process. *Protoplasma* **231**, 55–63 (2007).

27. Lowe, C. D., Minter, E. J., Cameron, D. D. & Brockhurst, M. A. Shining a light on exploitative host control in a photosynthetic endosymbiosis. *Curr Biol* **26**, 207–211 (2016).
28. Sørensen, M. E. S. *et al.* The role of exploitation in the establishment of mutualistic microbial symbioses. *FEMS Microbiol Lett* **366**, (2019).
29. Sørensen, M. E. S., Wood, A. J., Cameron, D. D. & Brockhurst, M. A. Rapid compensatory evolution can rescue low fitness symbioses following partner-switching. *bioRxiv* 2020.11.06.371401 (2020) doi:10.1101/2020.11.06.371401.
30. Axelrod, R. & Hamilton, W. D. The evolution of cooperation. *Science* **211**, 1390–1396 (1981).
31. Foster, K. R. & Wenseleers, T. A general model for the evolution of mutualisms. *J. Evol. Biol.* **19**, 1283–1293 (2006).
32. Frank, S. A. *Foundations of Social Evolution*. (Princeton University Press, 1998).
33. Herre, E. A., Knowlton, N., Mueller, U. G. & Rehner, S. A. The evolution of mutualisms: exploring the paths between conflict and cooperation. *Trends in Ecology & Evolution* **14**, 49–53 (1999).
34. Szathmáry, E. & Smith, J. M. The major evolutionary transitions. *Nature* **374**, 227–232 (1995).
35. West, S. A., Fisher, R. M., Gardner, A. & Kiers, E. T. Major evolutionary transitions in individuality. *PNAS* **112**, 10112–10119 (2015).
36. Buck, A. H. *et al.* Exosomes secreted by nematode parasites transfer small RNAs to mammalian cells and modulate innate immunity. *Nat Commun* **5**, 5488 (2014).

37. Guo, Z., Li, Y. & Ding, S. W. Small RNA-based antimicrobial immunity. *Nat Rev Immunol* **19**, 31–44 (2019).

38. Huang, C. Y., Wang, H., Hu, P., Hamby, R. & Jin, H. Small RNAs - big players in plant-microbe interactions. *Cell Host Microbe* **26**, 173–182 (2019).

39. Wang, M. *et al.* Bidirectional cross-kingdom RNAi and fungal uptake of external RNAs confer plant protection. *Nat Plants* **2**, 16151 (2016).

40. Weiberg, A. *et al.* Fungal small RNAs suppress plant immunity by hijacking host RNA interference pathways. *Science* **342**, 118–23 (2013).

41. Jenkins, B. H. *et al*. Characterization of the RNA-interference pathway as a tool for reverse genetic analysis in the nascent phototrophic endosymbiosis, *Paramecium bursaria*. *Royal Society Open Science* **8**, 210140.

42. Carradec, Q. *et al.* Primary and secondary siRNA synthesis triggered by RNAs from food bacteria in the ciliate *Paramecium tetraurelia*. *Nucleic Acids Res* **43**, 1818–33 (2015).

43. Galvani, A. & Sperling, L. RNA interference by feeding in *Paramecium*. *Trends Genet* **18**, 11–2 (2002).

44. Karunanithi, S. *et al.* Exogenous RNAi mechanisms contribute to transcriptome adaptation by phased siRNA clusters in *Paramecium*. *Nucleic Acids Res* **47**, 8036–8049 (2019).

45. Marker, S., Carradec, Q., Tanty, V., Arnaiz, O. & Meyer, E. A forward genetic screen reveals essential and non-essential RNAi factors in *Paramecium tetraurelia*. *Nucleic Acids Res* **42**, 7268–80 (2014).

46. Marker, S., Le Mouël, A., Meyer, E. & Simon, M. Distinct RNA-dependent RNA polymerases are required for RNAi triggered by double-stranded RNA versus truncated transgenes in *Paramecium tetraurelia*. *Nucleic Acids Res* **38**, 4092–107 (2010).

47. Karunanithi, S. *et al.* Feeding exogenous dsRNA interferes with endogenous sRNA accumulation in *Paramecium*. *DNA research : an international journal for rapid publication of reports on genes and genomes* **27**, (2020).
48. Cerutti, H., Ma, X., Msanne, J. & Repas, T. RNA-mediated silencing in algae: biological roles and tools for analysis of gene function . *Eukaryot Cell* **10**, 1164–1172 (2011).
49. Hoehener, C., Hug, I. & Nowacki, M. Dicer-like enzymes with sequence cleavage preferences. *Cell* **173**, 234-247.e7 (2018).
50. Ahmed, F. & Raghava, G. P. S. Designing of highly effective complementary and mismatch siRNAs for silencing a gene. *PLoS One* **6**, (2011).
51. Du, Q., Thonberg, H., Wang, J., Wahlestedt, C. & Liang, Z. A systematic analysis of the silencing effects of an active siRNA at all single-nucleotide mismatched target sites. *Nucleic Acids Res* **33**, 1671–1677 (2005).
52. Jackson, A. L. *et al.* Widespread siRNA "off-target" transcript silencing mediated by seed region sequence complementarity. *RNA* **12**, 1179–1187 (2006).
53. Doench, J. G., Petersen, C. P. & Sharp, P. A. siRNAs can function as miRNAs. *Genes Dev* **17**, 438–442 (2003).
54. Ameres, S. L., Martinez, J. & Schroeder, R. Molecular basis for target RNA recognition and cleavage by human RISC. *Cell* **130**, 101–112 (2007).
55. Kodama, Y. *et al.* Comparison of gene expression of *Paramecium bursaria* with and without *Chlorella variabilis* symbionts. *BMC Genomics* **15**, 183 (2014).
56. Cotton, J. A. & McInerney, J. O. Eukaryotic genes of archaebacterial origin are more important than the more numerous eubacterial genes, irrespective of function. *Proceedings of the National Academy of Sciences* **107**, 17252–17255 (2010).
57. Fujishima, M. & Kodama, Y. Endosymbionts in *Paramecium*. *Eur J Protistol* **48**, 124–37 (2012).

58. Matthews, J. L. *et al.* Partner switching and metabolic flux in a model cnidarian-dinoflagellate symbiosis. *Proc Biol Sci* **285**, (2018).

59. Matsuura, Y. *et al.* Recurrent symbiont recruitment from fungal parasites in cicadas. *PNAS* **115**, E5970–E5979 (2018).

60. Husnik, F. & McCutcheon, J. P. Repeated replacement of an intrabacterial symbiont in the tripartite nested mealybug symbiosis. *PNAS* **113**, E5416–E5424 (2016).

61. Hickey, D. A. Selfish DNA: a sexually-transmitted nuclear parasite. *Genetics* **101**, 519–531 (1982).

62. Kiers, E. T., Rousseau, R. A., West, S. A. & Denison, R. F. Host sanctions and the legume–rhizobium mutualism. *Nature* **425**, 78–81 (2003).

63. Hansen, D. R., Van Alfen, N. K., Gillies, K. & Powell, W. A. Naked dsRNA associated with hypovirulence of *Endothia parasitica* is packaged in fungal vesicles. *Journal of General Virology,* **66**, 2605–2614 (1985).

64. Zhang, J. D., Biczok, R. & Ruschhaupt, M. ddCt: The ddCt Algorithm for the Analysis of Quantitative Real-Time PCR (qRT-PCR). (Bioconductor version: Release (3.11), 2020). doi:10.18129/B9.bioc.ddCt.

65. Arriola, M. B. *et al.* Genome sequences of *Chlorella sorokiniana* UTEX 1602 and *Micractinium conductrix* SAG 241.80: implications to maltose excretion by a green alga. *The Plant Journal* **93**, 566–586 (2018).

66. Liu, P. *et al.* Complete genome sequence of *Klebsiella pneumoniae* subsp. pneumoniae HS11286, a multidrug-resistant strain isolated from human sputum. *J. Bacteriol.* **194**, 1841–1842 (2012).